DESY 96-074

Mixing angle of scalar mesons and kaon polarizability in a chiral quark σ-model

D. Ebert T. Feldmann, M. K. Volkov

Institut für Physik, Humboldt–Universität zu Berlin,
Invalidenstraße 110, D–10115 Berlin, Germany

Mixing angle of scalar mesons and kaon polarizability in a chiral quark σ-model

D. Ebert*, T. Feldmann‡, M. K. Volkov* †
Institut für Physik, Humboldt–Universität zu Berlin,
Invalidenstraße 110, D–10115 Berlin, Germany

Abstract

Using present data for the decays $f_0 \to \gamma\gamma$, $f_0 \to \pi\pi$, we determine the mixing angle of scalar mesons in a chiral quark σ-model. This value is employed for an analysis of the kaon polarizability. It is shown that pole diagrams from intermediate scalar mesons and their mixing angle significantly affect the electromagnetic polarizability of charged and neutral kaons. Our results are compared to other models and the results of the chiral symmetry limit.

*Supported by *Deutsche Forschungsgemeinschaft* under contract 436 RUS 113/29.
†On leave of absence of Joint Institute for Nuclear Research, Dubna, Russia.
‡Supported by *Deutsche Forschungsgemeinschaft* under contract Eb 139/1-2.

1 Introduction

There is a renewed interest in electromagnetic polarizabilities of the pion and kaon which together with other low-energy parameters like electromagnetic radii provide us with useful information on the internal structure of mesons (for a review on recent results obtained in different models see e.g. refs. [1, 2, 3]). Some of us calculated these polarizabilities earlier within nonlinear chiral hadron theories [4, 5] as well as on the basis of a bosonized NJL-model [6] leading to a linear σ-model [7, 8]. In the linear σ-model pole diagrams arising from intermediate scalar mesons[1] ϵ, $f_0(980)$ and $a_0(980)$ turn out to play an important role in the calculation of meson polarizabilities. In particular, for describing the physical isoscalar scalar mesons ϵ and f_0 within an underlying quark model, one has to take into account the mixing angle θ of the (u,d) and (s) quark content of these mesons (see [7]). In the latter paper strong and radiative decays of scalar mesons were investigated solely on the level of quark loop triangle diagrams.

In a recent paper [11] it was however argued that additional meson loop contributions play an important role for the description of the scalar meson decay $a_0(\delta) \to \gamma\gamma$. This idea does not contradict the usual $1/N_c$ expansion, since both quark and meson loops turn out to be of the same order in N_c for this case. Stimulated by these arguments we have recalculated the decay amplitudes of scalar mesons. As a result we find that in the case of $a_0 \to \gamma\gamma$ the additional effect of meson loops only weakly changes the result (an increase of about 16% with respect to [7]) in contrast to ref. [11]. There an effect of 50% was found, and quark and meson loops interfere in a destructive way, while we find both effects to be additive. On the other hand, pion and particularly kaon loops turn out to be indeed essential for the description of the decay $f_0 \to \gamma\gamma$, which is crucial for the determination of the mixing angle on the basis of new experimental data. We find a value $\theta = 23^\circ$ for the mixing angle, which would change to $\theta = -18^\circ$ if meson loops were omitted.

Clearly, changes of the mixing angle also significantly influence other physical quantities, like the kaon polarizability. Therefore, in the second part of this paper, we apply the new results to an estimate of the kaon polarizability.

2 Lagrangians and determination of the mixing angle

For definiteness, let us consider meson vertices generated by quark loops arising in the bosonization approach of QCD-motivated quark models [7, 6]. The corresponding local terms then satisfy approximate chiral symmetry of the resulting effective meson lagrangian in the case of $m_s \neq m_u$, where m_s, m_u are the constituent masses of strange or (u,d)-quarks, respectively. First, let us quote that part of the meson lagrangian which describes the decays of scalar mesons $\epsilon(700-750)$, $f_0(980)$ and $a_0(980)$ into two pions and kaons [8] (see Fig. 1a)

$$\begin{aligned} \mathcal{L}_1 &= \sum_{S=\epsilon,f_0} \Big(G_\pi^S \, \vec{\pi}^2(x)\, S(x) + G_K^S \, \bar{K}(x)\, K(x)\, S(x) \Big) \\ &\quad + G_K^{a_0} \, \bar{K}(x)\, \tau_3 \, K(x)\, a_0(x) \; , \end{aligned} \tag{1}$$

where

$$G_\pi^\epsilon = 2\, g_\pi \, Z^{1/2} \, m \, \cos\theta \; ,$$

[1] The ϵ meson is considered to be a broad resonance with a mass and width which are presently not yet completely fixed [9]. We shall use here a mass $M_\epsilon = 700 - 750$ MeV. The masses of the other scalar mesons are given by $M_{f_0} = 980$ MeV and $M_{a_0} = 983$ MeV [10].

$$
\begin{aligned}
G_\pi^{f_0} &= 2\, g_\pi\, Z^{1/2}\, m\, \sin\theta \ , \\
G_K^{\epsilon} &= 2\, g_K\, Z^{1/2}\, \left[(2m - m_s)\, \cos\theta + \sqrt{2}\,(2m_s - m)\, \sin\theta\right] \ , \\
G_K^{f_0} &= 2\, g_K\, Z^{1/2}\, \left[(2m - m_s)\, \sin\theta - \sqrt{2}\,(2m_s - m)\, \cos\theta\right] \ , \\
G_K^{a_0} &= 2\, g_K\, Z^{1/2}\, (2m - m_s) \ . \qquad (2)
\end{aligned}
$$

Besides of the Goldberger-Treiman relations $g_\pi = m/F_\pi$, $g_K = (m_u + m_s)/(2F_K)$, we shall use the following parameter values $F_\pi = 93$ MeV, $F_K = 1.2\, F_\pi$, $m_u = m_d = m = 280$ MeV, $m_s = 450$ MeV. Here Z is a renormalization coefficient arising from π-A_1-mixing ($Z \approx 1.4$ [7]).

Below we shall determine the mixing angle θ which describes the deviation of the singlet-octet mixing angle from ideal mixing by using recent experimental data for $f_0 \to 2\gamma$ and $f_0 \to 2\pi$. For this, we remind that the scalar components of ideal mixing are related to the physical meson states through

$$
\begin{aligned}
(\sigma_8 + \sqrt{2}\,\sigma_0)/\sqrt{3} &= \epsilon\, \cos\theta + f_0\, \sin\theta \ , \\
(\sqrt{2}\,\sigma_8 - \sigma_0)/\sqrt{3} &= f_0\, \cos\theta - \epsilon\, \sin\theta \ . \qquad (3)
\end{aligned}
$$

Let us next consider two-photon decays of scalar mesons which are described by finite quark and meson loop diagrams (see Fig. 1 b - d).

The amplitude of the decay $S \to 2\gamma$ arising from quark loops takes the form

$$
T^{q\mu\nu} = (g^{\mu\nu}\, q_1 q_2 - q_2^\mu\, q_1^\nu)\, T^q \ , \qquad (4)
$$

where

$$
T^q = \frac{a_S}{3}\, \frac{\alpha}{\pi F_\pi Z^{1/2}}\, x\, \left[\phi(x) - (x\,\phi(x) - 1)\right] \ . \qquad (5)
$$

Here $q_{1,2}$ are the photon momenta, $\alpha = 1/137$, $x_i = (2m_i^2)/(q_1 q_2) = (2m_i/M_S)^2$, and the coefficient a_S is given by

$$
\begin{aligned}
a_\epsilon &= 5\cos\theta + \sqrt{2}\,\frac{F_\pi}{F_S}\,\sin\theta \ , \\
a_{f_0} &= 5\sin\theta - \sqrt{2}\,\frac{F_\pi}{F_S}\,\cos\theta \ , \\
a_{a_0} &= 3 \ , \qquad (6)
\end{aligned}
$$

with $F_S = 1.28\, F_\pi$ [7]. Finally, the function $\phi(x)$ is defined by

$$
\phi(x) = \begin{cases} \left[\arctan(x-1)^{-1/2}\right]^2 \ , & x \geq 1 \\ \left[\frac{i}{2}\,\ln\frac{1-\sqrt{1-x}}{1+\sqrt{1-x}} - \frac{\pi}{2}\right]^2 \ , & x \leq 1 \ . \end{cases} \qquad (7)
$$

Considering the $f_0(a_0)$ meson, we have $x < 1$ so that, due to (7), there arises an imaginary part in the amplitude T_q. Such a contribution would describe the decay of a meson into a free $q\bar{q}$-pair, in obvious contradiction to quark confinement. Of course, this is an artefact of every quark model using unconfined quark propagators. The usual procedure to avoid this problem is to use a low-momentum expansion around $q_1 \cdot q_2 \approx 0$. In refs. [6, 7, 12] it was shown that such a prescription respects $SU(3)_F$-symmetry and leads to reasonable results for 2 photon decays of the pseudoscalar

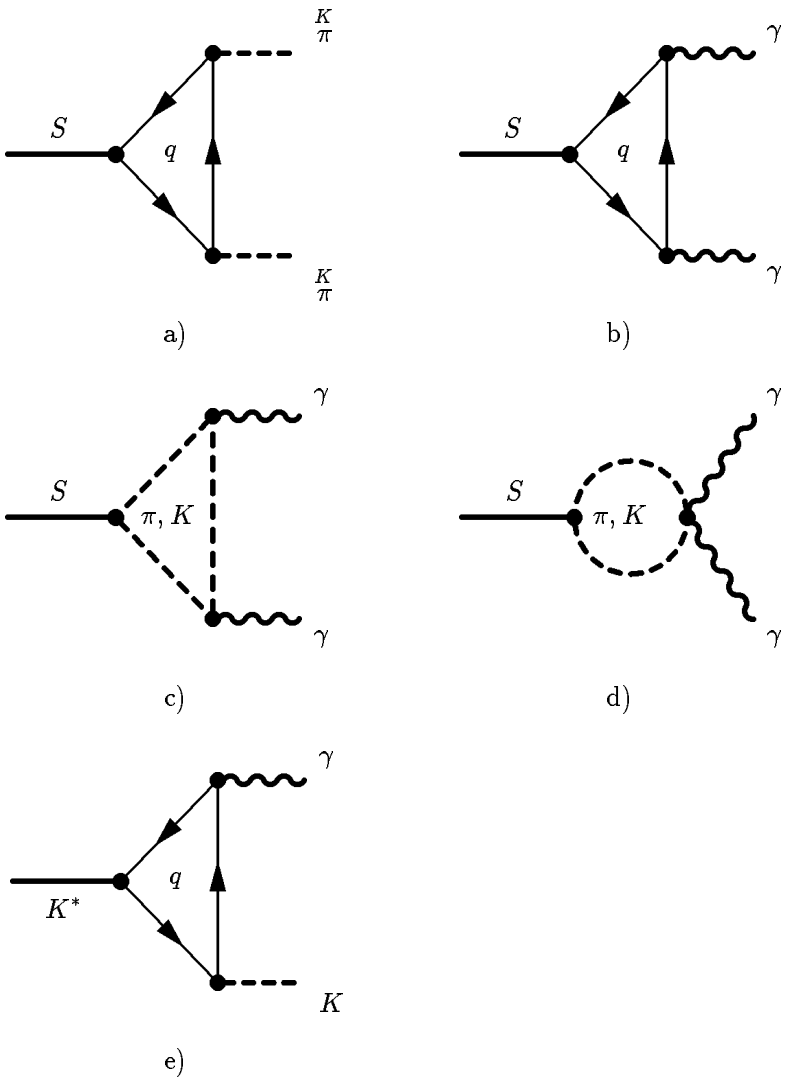

Figure 1: a,b) Quark triangle diagrams describing two-kaon(pion) and two-photon decays of scalar mesons $S = \{\epsilon, f_0, a_0\}$. c,d) Meson loop diagrams contributing to two-photon decays. e) Anomalous triangle diagram describing the radiative decay of K^* mesons.

meson nonet. In the low-momentum limit ($x \to \infty$) the amplitude (5) then leads to the simplified expression

$$T^q = \frac{2}{3}\frac{a_S}{3}\frac{\alpha}{\pi F_\pi Z^{1/2}} \ . \tag{8}$$

Let us next calculate the meson loop contributions of Figs. 1c,d) which, due to $G^S \sim g_S \sim 1/\sqrt{N_c}$, contribute in the same order of the $1/N_c$ expansion as the quark loop diagrams. Taking into account the Lagrangian of electromagnetic interactions

$$\begin{aligned}\mathcal{L}_2 &= i\,e\,A^\mu\left(\pi^-\,\partial_\mu\pi^+ - \pi^+\,\partial_\mu\pi^- + K^-\,\partial_\mu K^+ - K^+\,\partial_\mu K^-\right) \\ &\quad + e^2\,A_\mu^2\,(\pi^+\pi^- + K^+K^-)\ ,\end{aligned} \tag{9}$$

one easily obtains

$$T^{m\,\mu\nu} = (g^{\mu\nu}\,q_1q_2 - q_2^\mu q_1^\nu)\,T^m \ , \tag{10}$$

with

$$T^m = G_M^S\,\eta\,\frac{\alpha}{2\pi}\,\frac{2}{M_S^2}\,\left[\tilde{x}\,\phi(\tilde{x}) - 1\right] \ , \tag{11}$$

where $\tilde{x} = \frac{2M^2}{q_1\,q_2} = \left(\frac{2M}{M_S}\right)^2$, $\eta = 2(1)$ for pions (kaons), and M is the mass of the meson circulating in the loop. Note that the terms in the square bracket of the meson loop expression (11) differ in sign from the corresponding expressions in the quark loop amplitude (5) due to the usual minus sign coming from the closed fermion loop[2].

Let us next use these results for the determination of the mixing angle θ from the decays $f_0 \to \gamma\gamma$ and $f_0 \to \pi\pi$. Taking into account expressions (8), (11), the total amplitude for the decay $f_0 \to 2\gamma$ consisting of quark, pion and kaon loops, reads[3]

$$\begin{aligned}T_{f_0\to\gamma\gamma} &= T^q_{f_0\to\gamma\gamma} + T^\pi_{f_0\to\gamma\gamma} + T^K_{f_0\to\gamma\gamma}\ , \\ T^q_{f_0\to\gamma\gamma} &= \frac{\alpha}{\pi F_\pi}\,(-0.2\,\cos\theta + 0.9\,\sin\theta)\ , \\ T^\pi_{f_0\to\gamma\gamma} &= \frac{\alpha}{\pi F_\pi}\,(-0.4 + 0.2\,i)\,\sin\theta\ , \\ T^K_{f_0\to\gamma\gamma} &= \frac{\alpha}{\pi F_\pi}\,(-0.7\,\cos\theta + 0.1\,\sin\theta)\ , \\ T_{f_0\to\gamma\gamma} &= -0.9\,\frac{\alpha}{\pi F_\pi}\,\sin\theta\,(\cot\theta - 0.65 - 0.2\,i)\ .\end{aligned} \tag{12}$$

Now, using the Lagrangian $\mathcal{L}_1$ and the amplitude (12), we obtain the following expressions for the decay widths of $f_0 \to \gamma\gamma$ and $f_0 \to \pi\pi$

$$\Gamma_{f_0\to\gamma\gamma} = \frac{M_{f_0}^3}{64\pi}\,|T_{f_0\to\gamma\gamma}|^2 \ , \tag{13}$$

$$\Gamma_{f_0\to\pi\pi} = \frac{3Z}{2\pi M_{f_0}}\left(\frac{m^2}{F_\pi}\right)^2\sqrt{1 - \left(\frac{2M_\pi}{M_{f_0}}\right)^2}\,\sin^2\theta\ . \tag{14}$$

[2]Concerning the $a_0(\delta)$ meson, we find a different relative sign of quark and meson loop contributions than in ref. [11]. The K-meson loop slightly increases (16%) the result which comes out to be overestimated within the quark loop approach, anyway [7].

[3]Small contributions of loop diagrams with non-strange scalar mesons (10% of $T^\pi_{f_0\to\gamma\gamma}$) and strange scalar mesons (4% of $T^K_{f_0\to\gamma\gamma}$) will be omitted.

By comparing their ratio to the experimental value [10]

$$\frac{\Gamma_{f_0\to\gamma\gamma}}{\Gamma_{f_0\to\pi\pi}} \;=\; 1.5\cdot 10^{-5}\;, \tag{15}$$

we obtain two solutions, $\theta = 23^\circ$ and $\theta = -43^\circ$. The choice $\theta = 23^\circ$ leads to predictions

$$\Gamma_{f_0\to\gamma\gamma} = 1.1 \text{ keV}\;,$$

$$\Gamma_{f_0\to\pi\pi} = 72 \text{ MeV}\;,$$

which are somewhat larger than the averaged values of PDG [10]. It is worth mentioning that discarding meson loops would even yield a negative angle $\theta \sim -18^\circ$.

For later applications, let us also quote the effective Lagrangian describing the radiative decay $K^* \to K\gamma$ of vector mesons corresponding to the anomalous quark triangle diagram shown in Fig. 1e),

$$\mathcal{L}_3 \;=\; \frac{e\,g_V}{32\,\pi^2\,F_K}\,a_{K^*}\,\epsilon^{\sigma\kappa\nu\mu}\,F_{\kappa\nu}(x)\,K^*_{\sigma_\mu}(x)\,K(x)\;, \tag{16}$$

with $g_V = g_\rho$ being the vector meson coupling constant ($g_\rho^2/(4\pi) \approx 3$). Moreover, using the value of the quark mass ratio $\lambda = m_u/m_s \sim 0.6$, the coefficients a_{K^*} are estimated as [8]

$$\begin{aligned} a_{K^{*+}} &= \frac{1}{2}\left[1 - \frac{2\,\lambda}{1-\lambda^2}\left(3 + \frac{2+\lambda^2}{1-\lambda^2}\,\ln\lambda^2\right)\right] \simeq 1.2\;, \\ a_{K^{*0}} &= 1 - \frac{\lambda}{1-\lambda^2}\,\ln\lambda^2 \simeq 2\;. \end{aligned} \tag{17}$$

Finally, we need the box-diagram describing the low-energy Compton-effect off K mesons, shown in Fig. 2. This diagram leads to the Lagrangian term

$$\mathcal{L}_4 \;=\; \frac{\alpha}{18\pi\,F_K^2}\,F^2_{\mu\nu}(x)\,(K^+(x)\,K^-(x) + 4\,K^0(x)\bar{K}^0(x))\;. \tag{18}$$

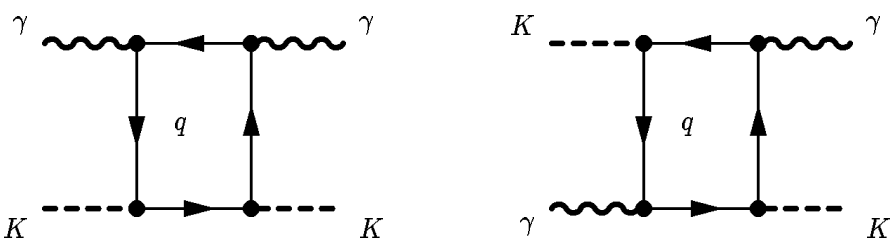

Figure 2: Quark box diagrams describing the low-energy Compton-effect off K mesons.

3 Kaon polarizability

In nonlinear chiral models [5] (arising in the limit $M_S \to \infty$) and in the chiral-symmetry limit of the linear σ-model [8] the main contributions to the polarizability of charged kaons and pions emerge from pole diagrams with intermediate scalar mesons containing the quark loop vertices

shown in Fig. 1a,b)[4]. This is contrary to the case of neutral mesons where the contributions of corresponding pole diagrams are completely cancelled by the box diagrams shown in Fig. 2.

Beyond the chiral limit, this situation still holds for pions, whereas for kaons the result strongly depends on the value of the mixing angle. We will find below that for $\theta = 23^\circ$ the scalar meson contribution to the charged kaon polarizability is reduced by about 50% with respect to the value of the chiral limit but still dominates the box diagram contribution. For neutral kaons the contribution of pole diagrams becomes slightly enhanced with respect to the box diagram term, leading to a small but non-vanishing value of the neutral kaon polarizability. To see this in more detail, let us write the contributions of scalar meson pole and box diagrams to the kaon polarizability $\alpha_K^{(S+b)}$ in the form[5]

$$\begin{aligned} \alpha_{K^+}^{(S+b)} &= C\,(2\,\Delta_+ - 1)\ , \\ \alpha_{K^0}^{(S+b)} &= C\,(2\,\Delta_- - 4)\ , \qquad C = \frac{\alpha}{18\pi\,F_K^2\,M_K}\ , \end{aligned} \tag{19}$$

where

$$\begin{aligned} \Delta_\pm &= (m_s + m)\left\{ \frac{a_\epsilon}{M_\epsilon^2}\left[(2m - m_s)\,\cos\theta + \sqrt{2}(2m_s - m)\,\sin\theta\right]\right. \\ &\quad -\frac{a_{f_0}}{M_{f_0}^2}\left[\sqrt{2}(2m_s - m)\,\cos\theta - (2m - m_s)\,\sin\theta\right] \\ &\quad \left. \pm\frac{a_{a_0}}{M_{a_0}^2}\,(2m - m_s)\right\}\ . \end{aligned} \tag{20}$$

Taking into account (6), $\theta = 23^\circ$ and using two different values of the ϵ-mass, $M_\epsilon = 700(750)$ MeV, we obtain $\Delta_+ = 3.04(2.60)$, $\Delta_- = 2.58(2.14)$. This leads to the following estimates

$$\begin{aligned} \alpha_{K^+}^{(S+b)} &\simeq C\,(6.78(5.90) - 1.16 + 0.46 - 1 = 6.08(5.20) - 1) = 8.2(6.8)\cdot 10^{-4}\,\mathrm{fm}^3\ , \\ \alpha_{K^0}^{(S+b)} &\simeq C\,(6.78(5.90) - 1.16 - 0.46 - 4 = 5.16(4.28) - 4) = 1.9(0.5)\cdot 10^{-4}\,\mathrm{fm}^3\ . \end{aligned} \tag{21}$$

For illustration, let us compare (21) with the results obtained in the chiral symmetry limit ($\theta = 0$, $M_\epsilon^2 = M_{f_0}^2 = M_{a_0}^2 \simeq 4m^2$). In this case we have

$$\begin{aligned} \alpha_{K^+}^{(S+b)} &\simeq C\,(5 + 2 + 3 - 1) = 14.5\cdot 10^{-4}\,\mathrm{fm}^3\ , \\ \alpha_{K^0}^{(S+b)} &\simeq C\,(5 + 2 - 3 - 4) = 0\ , \end{aligned} \tag{22}$$

where the first three terms in the brackets of (21,22) denote the pole contributions of ϵ, f_0 and a_0 mesons, whereas the last terms denote the contribution of the box diagrams. Thus, the deviation from chiral symmetry in combination with the above mixing angle influences the polarizability. From (21) and (22) we see that for $\theta = 23^\circ$ the contribution of the f_0-meson has not only decreased in absolute value but even has changed in sign compared to the chiral limit, whereas the a_0-contribution is reduced by an order of magnitude.

[4]The contribution of meson loop diagrams will be discussed later on (see Fig. 3).

[5]Recall that the electric and magnetic polarizabilities α_P, β_P of pseudoscalar mesons are obtained from the low-energy Compton amplitude by the decomposition

$$T_{NR} = -\vec{\epsilon}\cdot\vec{\epsilon}\,'\,\frac{\alpha}{M} + \vec{\epsilon}\cdot\vec{\epsilon}\,'\,\omega\omega'\,\alpha_P + (\vec{\epsilon}\times\vec{k})\cdot(\vec{\epsilon}\,'\times k')\,\beta_P$$

with ω (ω'), k (k') and ϵ ($\epsilon\,'$) being the incoming (outgoing) photon energy, momentum and polarization, respectively.

Scalar meson pole diagrams and box diagrams supply also analogous contributions to the magnetic polarizability $\beta_K^{(S+b)}$, but with opposite sign ($\alpha_K^{(S+b)} = -\beta_K^{(S+b)}$).

A large contribution to the magnetic polarizability of neutral kaons arises in addition from pole diagrams containing the intermediate vector meson K^*. It can easily be evaluated using the Lagrangian $\mathcal{L}_3$ which leads to the result

$$\beta_K^{(K^*)} = \left(\frac{a_{K^*}}{2\pi F_K}\right)^2 \frac{\alpha\, \alpha_V\, M_K}{M_{K^*}^2 - M_K^2} = \begin{cases} 4.4 \cdot 10^{-4}\,\mathrm{fm}^3 \ (K^+) \\ 12.2 \cdot 10^{-4}\,\mathrm{fm}^3 \ (K^0)\ . \end{cases} \tag{23}$$

For completeness, let us next consider the meson loop diagrams shown in Fig. 3 leading to

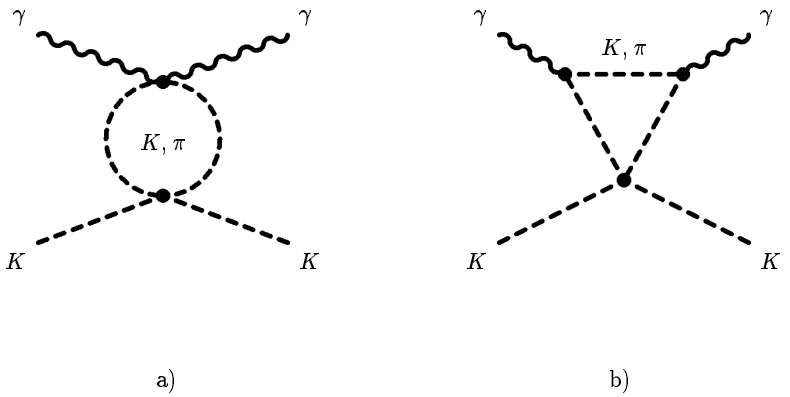

Figure 3: a,b) Meson loop diagrams contributing to the low-energy Compton-effect for K mesons and to the kaon polarizability.

additional contributions to the kaon polarizability comparable to the values obtained from (19). These contributions have been first evaluated in ref. [4] for a nonlinear chiral theory, providing a suitable low-energy approximation of the linear σ-model. The expression of the Compton-amplitude associated with the diagrams exhibited in Fig. 3 reads

$$\begin{aligned} T_\pm^{\mu\nu} &= \frac{2\alpha}{4\pi F_K^2}\,(g^{\mu\nu}\, q_1{\cdot}q_2 - q_1^\nu\, q_2^\mu)\,\left[\beta^{(\pi)}(q_1q_2) + \beta_\pm^{(K)}(q_1q_2)\right]\ , \\ T_0^{\mu\nu} &= \frac{2\alpha}{4\pi F_K^2}\,(g^{\mu\nu}\, q_1{\cdot}q_2 - q_1^\nu\, q_2^\mu)\,\left[\beta^{(\pi)}(q_1q_2) + \beta_0^{(K)}(q_1q_2)\right]\ . \end{aligned} \tag{24}$$

The function $\beta^{(\pi)}(q_1q_2)$ arising from the above two loop diagrams with internal pion lines is equal for charged and neutral kaons,

$$\beta^{(\pi)}(q_1q_2) = \frac{1}{2}\,[\tilde{x}_\pi\,\phi(\tilde{x}_\pi) - 1] \stackrel{q_1q_2\to 0}{\longrightarrow} 0\ . \tag{25}$$

The function $\beta_\pm^{(K)}$ describes the contribution of the loop diagrams of Fig. 3 with internal kaon propagators and external charged kaons,

$$\beta_\pm^{(K)} = \frac{1}{4}\,(\tilde{x}_K + 1)\,[\tilde{x}_K\,\phi(\tilde{x}_K) - 1] \stackrel{q_1q_2\to 0}{\longrightarrow} \frac{1}{12}\ . \tag{26}$$

For external neutral kaons we get

$$\beta_0^{(K)} = [\tilde{x}_K\,\phi(\tilde{x}_K) - 1] \stackrel{q_1q_2\to 0}{\longrightarrow} 0\ . \tag{27}$$

Thus, for $(q_1 \cdot q_2) = 0$ a nonvanishing contribution to the kaon polarizability arises only from $\beta_\pm^{(K)}(0) = 1/12$ leading to the result

$$\alpha_{K^\pm}^{(K)} = \frac{\alpha}{4\pi\, F_K^2\, M_K}\, \beta_\pm^{(K)}(0) \simeq 0.6 \cdot 10^{-4}\ \mathrm{fm}^3 = -\beta_{K^\pm}^{(K)}\ . \tag{28}$$

For neutral kaons the meson loop contribution to the polarizability vanishes.

We shall not calculate here the contributions of intermediate axial vector mesons (A) to the polarizability. The corresponding pole diagrams have been investigated in [7, 8],

$$\alpha_{K^\pm}^{(A)} = 0.9 \cdot 10^{-4}\ \mathrm{fm}^3\ , \qquad \alpha_{K^0}^{(A)} = 0.5 \cdot 10^{-4}\ \mathrm{fm}^3\ . \tag{29}$$

We mention that a noticeable contribution compared to the other terms was only obtained for the electric polarizability of charged kaons. Table 1 summarizes our estimates for the electric (α_K) and magnetic (β_K) polarizabilities as obtained from quark box diagrams (box), scalar meson pole diagrams (S), meson loop diagrams (M), intermediate vector (V) and axial vector (A) mesons. Thus, in comparision with the results of the chiral symmetry limit, for the realistic case of physical

	box	S	M	V	A	Total	chiral limit
α_{K^+}	- 1.6	9.8 (8.4)	0.6	0	0.9	9.7 (8.3)	16.0
α_{K^0}	- 6.5	8.4 (7.0)	0	0	0.5	2.4 (1.0)	0.5
β_{K^+}	1.6	-9.8 (-8.4)	-0.6	4.4	0	-4.4 (-3.0)	-10.7
β_{K^0}	6.5	-8.4 (-7.0)	0	12.2	0	10.3 (11.7)	12.2

Table 1: Electric and magnetic polarizabilities of kaons in units of 10^{-4} fm^3. The columns show the contributions from quark box diagrams (box), scalar meson poles (S), meson loops (M) and intermediate vector (V) and axial vector (A) mesons. The pole contributions are estimated for two values of the ϵ-mass, $M_\epsilon = 700(750)$ MeV.

scalar meson masses and a mixing angle $\theta = 23^\circ$ a slightly increased value of the electric polarizability should be observed for neutral kaons, whereas the electric and magnetic polarizabilities for charged kaons are reduced. For future comparision with data let us also quote the sum of the electric and magnetic kaon polarizabilities

$$\begin{aligned} (\alpha+\beta)_{K^+} &= 5.3 \cdot 10^{-4}\ \mathrm{fm}^3\ , \\ (\alpha+\beta)_{K^0} &= 1.3 \cdot 10^{-3}\ \mathrm{fm}^3\ . \end{aligned} \tag{30}$$

Note that our results satisfy the requirement $(\alpha+\beta)_K > 0$ from dispersion relations [1].

4 Summary and Conclusions

In this paper we have estimated the mixing angle of scalar mesons within a chiral quark σ-model from the decays $f_0 \to \gamma\gamma$, $f_0 \to \pi\pi$ by using new data [10] and taking into account both quark and meson loop diagrams. The new value of the mixing angle $\theta = 23^\circ$ obtained by including meson loops, significantly differs from the value $\theta = -18^\circ$ which would have been obtained if only quark loops were taken into account. The value $\theta = 23^\circ$ is then used to estimate the polarizability of kaons. For this aim we have calculated the low-energy Compton amplitude for K mesons,

taking into account scalar pole diagrams as well as box and triangle diagrams including quark and meson loops. As Table 1 shows, scalar meson poles give an important contribution to the electric and magnetic polarizabilities of charged and neutral mesons. The dominant scalar meson contributions arise here from the ϵ and f_0, whereas the contribution of the a_0 is relatively small. In this way, although the here obtained estimate for the amplitude $a_0 \to \gamma\gamma$ is overestimated by a factor 2 compared to experiment, the related error in the pole contributions to the charged kaon polarizabilities is only 5%.

Notice that our model allows one to study the deviation from the chiral symmetry limit ($M_\epsilon = M_{f_0} = M_{a_0} = 2m$; $\theta = 0$). As we find, for the realistic case of physical scalar meson masses and a mixing angle $\theta = 23^\circ$ the absolute values of the electric and magnetic polarizabilities for charged kaons are reduced by about 50%, whereas the electric polarizability of neutral kaons is increased. In the latter case the results turn out to be rather sensitive to changes of the ϵ-mass.

It is interesting to compare our result to predictions of other models. For example, the results of the Quark Confinement Model (QCM) [13] for the charged pion polarizability are close to the predictions of our model in ref. [8, 14], whereas they are larger by a factor 2–4 in the case of the kaon polarizability. An analogous result as in [13] was obtained for neutral kaons in an $SU(3)$ NJL-model [15].

In conclusion, we emphasize that just because different models lead to different results for the kaon polarizabilities, experimental verification of these predictions is an urgent and interesting task.

One of the authors (M.K.V.) would like to thank the particle theory group of the Humboldt University for the kind hospitality. This work was partially supported by the European Community via INTAS (94-2915).

References

[1] J. Portoles and M.R. Pennington, Preprint University of Durham, DTP-94/52 (1994).

[2] S. Bellucci, *Proceedings of Chiral Dynamics* Workshop at MIT (1994), ed. by A.M. Bernstein and B.R. Holstein, Springer Berlin, Heidelberg (1995).

[3] J. Gasser, *Proceedings of Chiral Dynamics* Workshop at MIT (1994), ed. by A.M. Bernstein and B.R. Holstein, Springer Berlin, Heidelberg (1995).

[4] M.K. Volkov and V.N. Pervushin, Sov. J. Nucl. Phys. **22** (1975) 179; Phys. Lett. **B55** (1975) 405; ibid. **B58** (1975) 177; Nuovo Cim. **27** (1975) 277.

[5] D. Ebert and M.K. Volkov, Phys. Lett. **B101** (1981) 252.

[6] D. Ebert and M.K. Volkov, Sov. J. Nucl. Phys. **36** (1982) 736; Z. Phys. **C16** (1983) 205.
M.K.Volkov, Ann. Phys. **157** (1984) 282.
D. Ebert and H. Reinhardt, Nucl. Phys. **B271** (1986) 188.

[7] M.K. Volkov, Sov. J. Part. and Nucl. **17** (1986) 186.

[8] M.K. Volkov, and A.A. Osipov, Sov. J. Nucl. Phys. **41** (1985) 659.

[9] G.Z. Mennessier, Z. Phys. **C16** (1983) 241;
M. Svec, A. de Lesquen and L. van Rossum, Phys. Rev. **D46** (1992) 949;
M. Svec, hep-th/9511205 (1995).

[10] Review of Part. Properties, Phys. Rev. **D50** (1994), 1173.

[11] A.S. Deakin, V. Elias, D.G.C. McKeon and M.D. Scadron, Mod. Phys. Lett. **A9** (1994) 2381.

[12] D. Ebert, H. Reinhardt and M.K. Volkov, in A. Faessler (ed.): Prog. Part. Nucl. Phys. **33** (1994) 1.

[13] M.A. Ivanov and T. Mizutani, Phys. Rev. **D45** (1992) 1580.

[14] A.E. Dorokhov, M.K. Volkov, J. Hüfner, S. Klevansky and P.Rehberg, Preprint University Heidelberg HD-TVP-95-12 (1995).

[15] V. Bernard and D. Vautherin, Phys. Rev. **D40** (1989) 1615.